HNPS Advances in Nuclear Physics

Vol 16 (2008)

HNPS2008

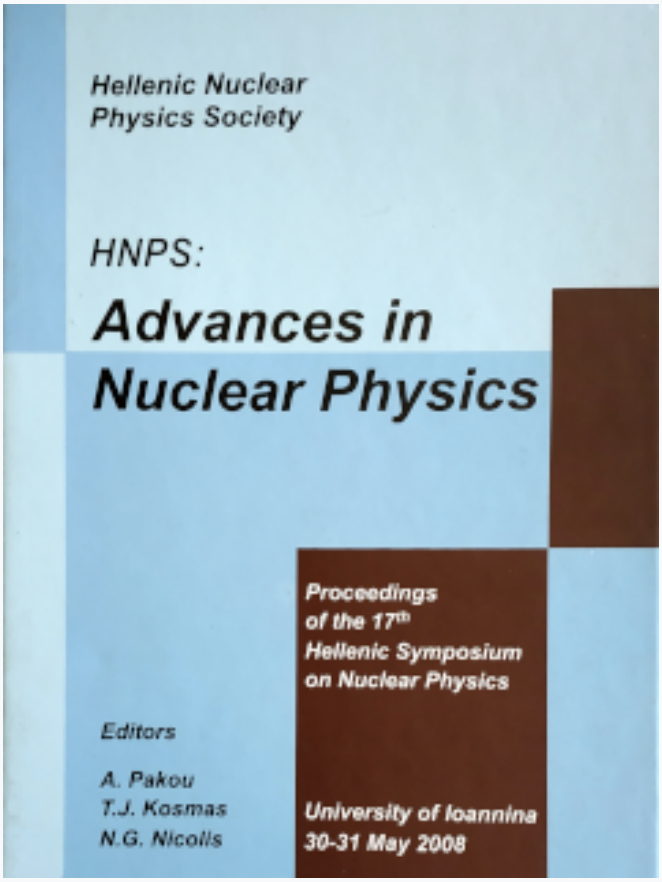

Novel radiation sources using relativistic electrons - Applications

A. Karabarbounis, Ch. Trikalinos, I. Papadakis, S. Sarros

doi: 10.12681/hnps.2578

Novel radiation sources using relativistic electrons - Applications

A. Karabarbounis [a,c], Ch. Trikalinos [b], I. Papadakis [a], and S. Sarros [a]

[a] *Department of Physics, National and Kapodistrian University of Athens, 15771 Athens, Greece*
[b] *Department of Methodology, History and Theory of Science, National and Kapodistrian University of Athens, 15771 Athens, Greece*
[c] *Institute of Accelerating Systems and Applications (IASA), Athens, Greece*

Abstract

Novel sources of radiation using relativistic electrons in periodic structures are being briefly discussed based on different mechanisms and producing radiation of very different characteristic.
In this article we will focus among others on the Smith-Purcell effect and the many efforts made since their discovery 55 years ago. Especially Smith-Purcell (SP) free-electron lasers (FELs) using low energy electron beam are being seen as attractive option for a compact source of coherent terahertz radiation. The latter refers to the production of radiation in the THz gap region associated with many applications including very promising and interesting results on imaging techniques in Medicine as well as applications in Biology, Molecular Physics etc. We will present calculations of Radiation Factors based on the Smith-Purcell radiation production with very interesting characteristics and discuss the possibility of calculating and designing a complete system of coherent THz radiation production based on a Smith-Purcell FEL.

---

1. Introduction

The discovery of Synchrotron Radiation (SR) followed the interaction of relativistic electrons with materials. They have been studied theoretically and experimentally, but it is only recently they have been considered as useful sources of radiation. We refer to Radiations from Relativistic Electrons in Periodic Structures (RREPS), namely Smith-Purcell (SP) Radiation [1], Parametric X-Ray (PXR), Coherent Bremsstrahlung (CB), Channeling Radiation (ChR), Transition Radiation (TR) as compare to Synchrotron Radiation.

The above phenomena can produce coherent and monochromatic radiation in the range below eV up to tens of keV, depending on the case, with excellent photon characteristics, an energy range of great interest for many applications. Another very important parameter refers to their brilliance and photon flux as compared to SR values.

In our days the excellent quality of new electron linacs, their very low emmitance, low background noise, along with their stability and high production rate guarantee their characteristics and feasibility to use them in small scale facilities. In Table 1 we present novel sources of radiation compared to a typical Synchrotron Radiation (SR) source. We see that in both cases either production from the electron itself or production of radiation from the media interacting with the electrons we have quite comparable numbers in brilliance or photon flux to SR radiation.

Novel sources of radiation can contribute to many applications as for example for MAD Protein Crystallography for modest size cells, SAXS & WAXS for polymers and proteins, Powder Diffraction with extreme environment, Chemical (small molecule) Crystallography, Photoelectron Spectroscopy of gases and solids, Spectromicroscopy, Magnetic X– ray CD, IR Spectromicroscopy, UV CD for Biology, EXAFS, Micro – Diffraction, Protein studies in the THz gap and imaging techniques [2] etc.

Table 1: Novel sources of radiation compared to Synchrotron Radiation [3]

Source	Electron energy	Photon energy	Flux in $\Delta\omega$ Photons/s	Collim. angle	Brilliance Ph/s mrad^2 mm^2 0.1bdw
SR - Bend Magnet	0.5-6 GeV	~ 100 keV	10^{12}-10^{13}	γ^{-1} vert	10^{13}-10^{14}
WIGGLER	0.2-6 GeV	~ 100 keV	10^{14}-10^{16}	γ^{-1} vert	10^{15}-10^{17}
UNDULATOR	0.2-6 GeV	~ 100 keV	10^{11}-10^{16}	1/10 γ^{-1}	10^{11}-10^{18}
SP	1-20 MeV	<1 eV	10^{11}-10^{13}	1 mrad	10^{8}
CB	10-200 MeV	1-100 keV	~10^{9}	1/3 γ^{-1}	10^{6}
ChR	10-200 MeV	1-100 keV	10^{9}-10^{11}	1/3 γ^{-1}	10^{7}-10^{8}
TR	50-900 MeV	0.1-100 keV	10^{11}-10^{13}	γ^{-1}	10^{13}-10^{15}
PXR	5-900 MeV	0.5-100 keV	10^{9}-10^{11}	5 mrad	10^{8}-10^{10}

In what follows we will focus only on the Smith-Purcell (SP) effect. It seams that there are many important applications to use this mechanism since SP radiation can produce intense radiation in a very large area of spectrum and especially from the far infrared (FIR) to the THz gap region (0.001-0.01 eV).

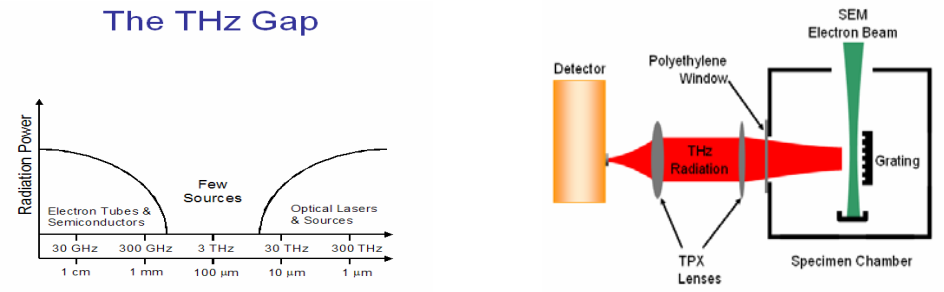

Fig. 1 The THz gap region and a simplified scheme of THz production (SP) [4]

The theory of Smith-Purcell effect

Relativistic electron beams (REB) can be used to produce Smith-Purcell (SP) radiation [1]. A rigorous theoretical solution for the SP radiation intensity depending on the metal grating profile and REB parameters is related to the calculation of the radiation factors. The theory of SP effect was carried out by describing the electric field of the moving electron in terms of evanescent plane waves. The diffraction of these waves produces the outgoing Smith-Purcell (SP) radiation.
A typical experimental layout for the study of SP mechanism is shown in Fig. 2. It refers to a laminar grating. In short the main parameters are the geometrical characteristics of the conductive grating (periodicity, D, how deep the grating is as compared to this and how far from the grating, the d value, the electron beam travels). Very important parameter remains the emmitance of the electron beam (see for example the technique used at Mainz -X1 group - to improve this problem).

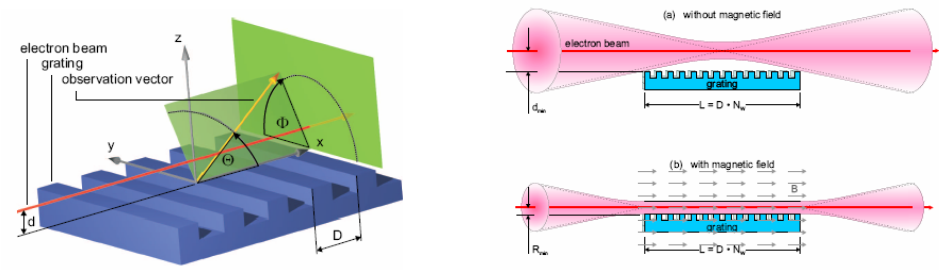

Fig. 2 Schematic layout of geometry of a SP experiment and the emmitance problem

The study of various kinds of gratings results to very different characteristics of radiation (radiation factors, spectral distribution etc). We will examine the case of triangular gratings (see Figure 3).

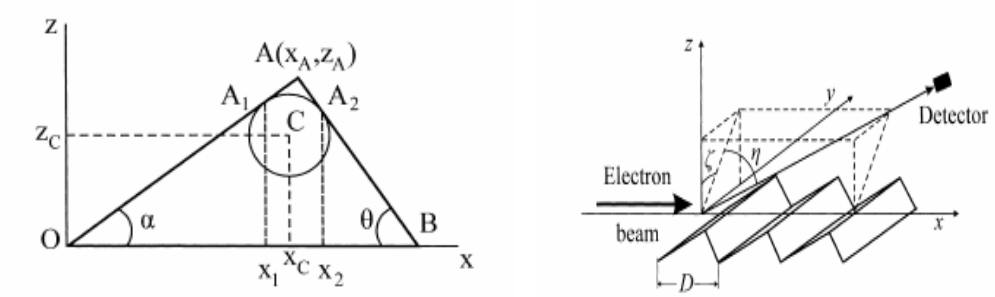

Fig. 3 The triangular grating and the parameters involved to our analysis

The method of modal expansion has been frequently applied to the diffraction problem. Rayleigh assumed that the “infinite series” representation for the diffracted field is valid on the boundary surface itself. This is called the Rayleigh assumption for the method of modal expansion. This assumption has frequently been questioned and criticized because the “infinite series” diverges and the Point Matching Method (PMM) [5] doesn’t give always a desirable solution.

Our purpose is to present a proper treatment of the PMM by adding smoothing procedures which lead to a reliable solution for the diffraction problem. Numerical results of the radiation factor in H-polarization case for triangular and blazed gratings are presented. Metal gratings with period in the millimeter range and REB with energy in 1-50 MeV domains were considered.

In H-polarization ($H_y \neq 0, E_y = 0$), Fourier components of the magnetic diffracted field are $H_y^d = H_y - H_y^i$, where H_y is the total magnetic field and H_y^i is the incident magnetic field. The diffracted field H_y^d satisfies the Helmholtz equation:

$$\partial_x^2 H_y^d + \partial_y^2 H_y^d + (k_0^2 - k_{y0}^2) H_y^d = 0\,, \qquad (1)$$

which is solved with the boundary condition $\vec{n}\nabla H_y = 0$ on the grating surface. Above the grating surface the diffracted field can be represented as a Rayleigh expansion that describes the field in terms of propagating and evanescent waves:

$$H_y^d(x,z;k_{yn},\omega) = \sum_{n=-\infty}^{+\infty} H_{yn}^d(k_{yn},\omega)\exp[i\cdot(\alpha_n x + \gamma_n z)]\,, \qquad (2)$$

where $\alpha_n = k_{xn}$ and $\gamma_n = k_{zn} = (k_0^2 - k_{yn}^2 - \alpha_n^2)^{1/2}$.

In order to find the magnetic field an analogous procedure followed by Ikuno and Yasuura [6] for diffraction of light calculations was used. The truncated expression of H_y^d is:

$$H_y^d(x,z;k_{yn},\omega) = \sum_{n=-N}^{+N} H_{yn}^d(N;k_{yn},\omega)\exp[i\cdot(\alpha_n x + \gamma_n z)]\,, \qquad (3)$$

in which 2*N*+1 is the number of harmonics taken into account.
Applying the Least Square Method for H_y^d and H_y^i one can obtain that:

$$\lim_{N\to\infty}\int\left|\vec{n}\nabla(H_y^i + H_y^d\right|^2 ds = 0, \quad \text{and} \quad \lim_{N\to\infty} H_{yn}^d(N;k_{yn},\omega) = H(k_{yn},\omega) \qquad (4)\,,\,(5)$$

where $\vec{n}$ is the unit vector normal to the grating surface.
By minimizing the right hand quantity from equation (4), a 2*N*+1 linear system of equations is obtained and it can be expressed in the form of a matrix equation $M_{pn} \times H_{yn}^d = V_p$. This related to the so called Improve Point Matching Method (IPMM) [7]. In the case of H-polarization the matrix elements are obtained as:

$$M_{pn} = \int_L \frac{[i\alpha_n g'(x) - i\gamma_n][i\alpha_p g'(x) - i\gamma_p]^*}{[1+g'(x)^2]} \exp\left\{i(-p)\frac{2p}{\lambda_g},+i(\gamma_n - \gamma_p^*)g(x)\right\} ds, \qquad (6)$$

$$V_p = \int_L \frac{[i\alpha_0 g'(x) - i\gamma_0][i\alpha_p g'(x) - i\gamma_p]^*}{[1+g'(x)^2]} \exp\left\{i(-p)\frac{2p}{\lambda_g}x + i(\gamma_0 - \gamma_p^*)g(x)\right\} ds, \qquad (7)$$

in which *n*, *p* are from –*N* to +*N*. Solving this system H_{yn}^{d} is found and the radiation factor $\left|R_n(\beta,\eta,0)\right|^2 = 4\exp\left(2\,|\,\gamma_o\,|\,z_o\right)\left\{(\varepsilon_o/\mu_o)\,|\,\mathrm{E}_{y,n}^{d}\,|^2 + |\,H_{y,n}^{d}\,|^2\right\}/e^2$ for the angles of emission η and ζ of a SP diffraction order n, with e^- the electron charge and $\gamma_0 = i(\alpha_o^2 + \beta^2 + K_o^2)^{1/2}$. The term is introduced in order to compensate the z_o dependence of $E_{y,n}^{d}$ and $H_{y,n}^{d}$. With this definition, the radiation factor does not depend on the distance z_o of the electron trajectory to the grating surface.

The IPMM is a procedure first presented by Ikuno and Yasuura [5, 6, 8] and it is a simple and general algorithm including the accuracy cheeks of the solution. In order to apply this method to a non-analytic profile of the grating (as the triangular one) it is necessary to eliminate the singularity points that are involved in the calculus.
In Figure 3 the schematic configuration of one grating period is presented and the experimental setup system of coordinates, including the triangular metal grating, the system of axis, the angles η and ζ, the position of the detector and the incident electron beam along the x-axis [9].

The triangular profile *OAB* (see Fig. 3) is approximated with the profile OA_1A_2B by replacing the top of the grating with a circle arc. The center of the circle is the *C* point of $(x_C,\ z_C)$ coordinates. In the points A_1 and A_2 the circle is tangent to the *OA* and *AB* segments, respectively.
In this way the initial non-continuous function which describe the triangular profile:

$$f(x) = \begin{cases} x\cdot\tan\alpha & \text{when} \quad x\in(0,x_A] \\ (\lambda_g - x)\cdot\tan\theta & \text{when} \quad x\in(x_A,\lambda_g] \end{cases}, \tag{8}$$

becomes:

$$g(x) = \begin{cases} x\cdot\tan\alpha & \text{when}\ \ x\in[0,x_1] \\ z_C + \sqrt{r^2-(x-x_C)^2} & \text{when}\ \ x\in[x_1,x_2] \\ (\lambda_g - x)\cdot\tan\theta & \text{when}\ \ x\in[x_2,\lambda_g] \end{cases}, \tag{9}$$

in which, *r* is the radius of the circle given by the function:

$$g_C(r,x) = z_C + \sqrt{r^2-(x-x_C)^2}\,, \tag{10}$$

In this way the singularity point *A* is eliminated by connecting the slopes α and θ with a smoothing function. Imposing the continuity conditions of $g(x)$ and its derivative $g'(x)$ in the points A_1 and A_2, and assuming that the connecting range $\Delta x = x_2 - x_1$ is very small (i.e. $\Delta x \le 1/100$ mm for λ_g in the millimeter domain) the center coordinates (x_C, z_C), the circle radius *r*, x_1 and x_2 can be determined from a linear system of 5 equations.
In this case the matrix elements M_{pn} and V_p from (6) and (7) respectively, become:

$$M_{pn} = I_1 + I_2 + I_3$$
$$V_p = J_1 + J_2 + J_3 \qquad (11)$$

in which:

$$I_1 = \int_{OA_1} \frac{\left[i\alpha_n \tan\alpha - i\gamma_n\right]\cdot\left[i\alpha_p \tan\alpha - i\gamma_p\right]^*}{\left[1+\tan^2\alpha\right]} \exp\left\{i(n-p)\frac{2p}{\lambda_g}\cdot x + i\left(\gamma_n - \gamma_p^*\right)\cdot x\tan\alpha\right\} ds \quad (12)$$

$$I_2 = \int_{A_1A_2} \frac{\left[i\alpha_n \frac{(x-x_C)}{\sqrt{r^2-(x-x_C)^2}} - i\gamma_n\right]\cdot\left[i\alpha_p \frac{(x-x_C)}{\sqrt{r^2-(x-x_C)^2}} - i\gamma_p\right]^*}{\left[1+\frac{(x-x_C)^2}{r^2-(x-x_C)^2}\right]} \exp\left\{i(n-p)\frac{2p}{\lambda_g}x + i\left(\gamma_n - \gamma_p^*\right)\cdot\left[z_C + \sqrt{r^2-(x-x_C)^2}\right]\right\} ds \quad (13)$$

$$I_3 = \int_{A_2B} \frac{\left[-i\alpha_n \tan\theta - i\gamma_n\right]\cdot\left[-i\alpha_p \tan\theta - i\gamma_p\right]^*}{\left[1+\tan^2\theta\right]} \exp\left\{i(n-p)\frac{2p}{\lambda_g}\cdot x + i\left(\gamma_n - \gamma_p^*\right)\cdot\left(\lambda_g - x\right)\cdot\tan\theta\right\} ds \quad (14)$$

and:

$$J_1 = \int_{OA_1} \frac{\left[i\alpha_0 \tan\alpha + i\gamma_0\right]\cdot\left[i\alpha_p \tan\alpha - i\gamma_p\right]^*}{\left[1+\tan^2\alpha\right]} \times \exp\left\{i(-p)\frac{2p}{\lambda_g}\cdot x + i\left(-\gamma_0 - \gamma_p^*\right)\cdot x\tan\alpha\right\} ds, \quad (15)$$

$$J_2 = \int_{A_1A_2} \frac{\left[i\alpha_0 \frac{(x-x_C)}{\sqrt{r^2-(x-x_C)^2}} - i\gamma_0\right]\cdot\left[i\alpha_p \frac{(x-x_C)}{\sqrt{r^2-(x-x_C)^2}} - i\gamma_p\right]^*}{\left[1+\frac{(x-x_C)^2}{r^2-(x-x_C)^2}\right]} *$$

$$\exp\left\{i(-p)\frac{2p}{\lambda_g}x + i\left(-\gamma_0 - \gamma_p^*\right)\cdot\left[z_C + \sqrt{r^2-(x-x_C)^2}\right]\right\} ds \quad (16)$$

$$J_3 = \int_{A_2B} \frac{\left[-i\alpha_0 \tan\theta - i\gamma_0\right]\cdot\left[-i\alpha_p \tan\theta - i\gamma_p\right]^*}{\left[1+\tan^2\theta\right]} \exp\left\{i(-p)\frac{2p}{\lambda_g}\cdot x + i\left(-\gamma_0 - \gamma_p^*\right)\cdot\left(\lambda_g - x\right)\cdot\tan\theta\right\} ds \quad (17)$$

The integrals I_1, I_3, J_1 and J_3 can be analytically solved by making the assumption for shallow grating profile $ds \cong dx$ which imply $h \le 0.25\lambda_g$ and the validity of the Rayleigh expansions (2). Integrals I_2 and J_2 were numerically integrated with a FORTRAN subroutine using a globally adaptive scheme based on Gauss-Kronrod rules. Then, the linear system of equations were solved using an iterative refinement algorithm,

increasing the size of the system matrix up to 120x120 for which convergence was observed.

This method allows the calculation the Radiation factors of the SP radiation for observation angles $\eta \le 45^o$ where reliable solutions were obtained. Often the numerical calculation failed due to the involvement of large size order of the linear matrix system.
Radiation factors of SP radiation generated by REB and triangular metal gratings were calculated with adapted IPMM. To perform the calculations the grating period was taken in millimeter and sub-millimeter domain and energies of the REB in 1 MeV to 50 MeV range. The radiation factors of SP radiation emitted in first negative order of diffraction (n=-1) were calculated in H-polarization, because they give the main contribution to the total emitted radiation. Figure 4 presents Radiation factor versus the angle η of observation for a triangular and a blazed grating respectively ($\alpha = 5^o$, $\theta = 35^o$ and $\theta = 85^o$) both with the period λ_g = 1.285 mm at 10 MeV. Obviously the groove heights are different, h = 0.11 mm for the blazed grating and h = 0.10 mm for the other one. The data for the blazed grating have been multiplied by a factor of 10^{-2} in order to emphasize the difference between the two dependencies. In this figure we see for the grating characterized by the angles (5^o, 35^o) that the peak near η =30° is enlarged and the Radiation factors are significantly increased after η =25°. In Figure 5 we present Radiation factors of SP radiation emitted in −1 order of diffraction versus angle of observation η, for a blazed grating with blaze angle $\alpha = 15^o$, and electron energies of 15 MeV and 50 MeV respectively. The period of the grating was λ_g = 5 mm and the groove height h = 1.25 mm which means that the ratio $h/\lambda_g = 0.25$, therefore, the Rayleigh assumption is valid. We can see in this figure that an increase in the groove height leads to the smoothness of the radiation factor dependencies on the angle η of observation, and that an increase of the electron energy implies a decrease in the radiation factor values.

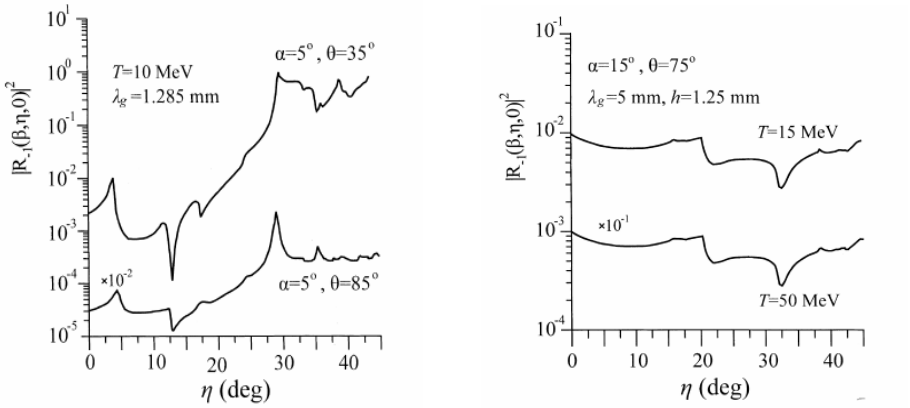

Fig. 4 Radiation factors for blazed and triangular gratingσ, for various angles, versus η

Experimental Setup

Taking in account these theoretical results, the practical manufacture of the metal grating seems to be a very important procedure due to the fact that the grating period and the groove height strongly affect the intensity of the emitted SP radiation. Using shallow

gratings and electron beams with energies up to 10 MeV the theory shows that the intensity of SP radiation will be higher than in the case of deeper gratings and larger electron energies.

An appropriate experimental setup should include an adequate vacuum chamber, containing the metal grating (MG), an optical system with the plane and parabolic off-axis mirror, a stepping motor driven movement mechanism of the plane mirror (translation and rotation). It will also need to have an appropriate window for the incoming and outgoing electron beam as well as a window for the produced SP radiation to the detector that is sitting outside the vacuum chamber.

Results from a Monte Carlo analysis were very useful to fix the sensitivity of the main parameters of the detecting system, the data acquisition and movement of the plane mirror. We expect a SP Radiation at the FIR region up to the THz gap region. Especially in the THz region there are very promising capabilities as an alternative imaging source. In Table 2 we present important parameters of various commercial and emerging research medical imaging modalities. We see that THz pulsed imaging or spectroscopy have very encouraging figures, especially in the data acquisition time and reconstruction, spatial resolution and sensitivity.

Table 2. Comparison of commercial and emerging medical imaging modalities including the THz pulsed imaging and spectroscopy [2]

	Planar X-ray	X-ray CT	Gamma camera image	Gamma camera SPECT	PET	Ultrasound B-scan + Doppler image	MRI image	MRI spectrum	Hyperpolarised MRI	Thermogram	OCT	Terahertz Pulsed Imaging	Terahertz Spectroscopy
Ionising radiation?	Yes	Yes	Yes	Yes	Yes	No	No	No	No	No	No	No	No
Anatomy or functional	A	A	F	F	F	A+F	A+F	F	F	F	A(+F)	A+F	F
Data acquisition time	<1 s	few s	5 min	20min	20min	1 s	20min	20min	1 s	<<1 s	10 s	1 min	<1s
Data reconstruction + process time	2 min	2 min	<1 s	10min	10min	< 1 s	2 min	< 1 s	< 1 s	<< 1 s	<1 s	< 1 s	< 10 s
Patient handling time	5 min	30min	10min	30min	30min	10min	1 hr	>1hr	10min	10min	10min	10min	10min
Spatial resolution	<1mm	>1mm	>5mm	>5mm	>5mm	>30μm	>1mm	>1mm	>1mm	>1mm	>15μm	>20μm	>20μm
Depth	>body	>body	>body	>body	>body	>body	>body	>body	>body	3mm	3mm	3mm	3mm
Sensitivity (1 poor to 5 great)	2	4	2	3	4	3	4	2	4	4	3	4	5
Availability of equipment in NHS hospitals (1 poor to 5 good)	5	2	3	2	1	5	1	1	1	2	2	1	1
Capital cost of equipment	£70k	£500k	£300k	£200k	£0.5-2M	£10k	£0.8k	£1.5M	£0.9M	£50k	<£50k	£250k	£250k

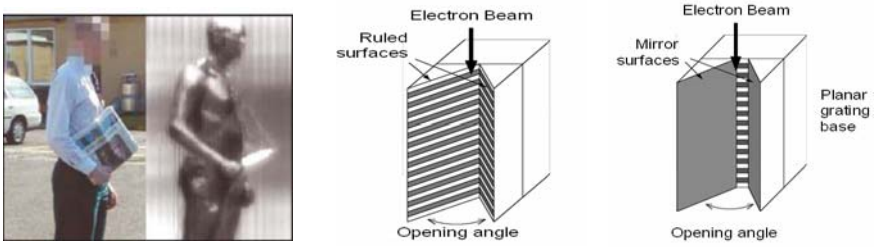

Fig 4 Imaging in the THz region and MG geometries to improve SP intensity [10,4]

Conclusions

The purpose of this work is to establish an optimum meta grating and relativistic electron beam parameters for the study of SP radiation. In order to measure the power of the emitted SP radiation it is necessary to know the angles η at which the strong coherent photons appear.

The numerical solution of IPMM for triangular and blazed metal gratings shows that this method supports the Rayleigh assumption while the PMM does not. The validity of the Rayleigh assumption is not related to the nature of the incoming wave (evanescent in the SP diffraction case, propagative in spectroscopy) but only to the grating profile. For grating profiles which are not analytic (i.e. triangular gratings) the Rayleigh assumption, combined with the PMM, is in general not correct, its validity being linked to the singularities of a conformal mapping. Therefore, to use PMM to these kinds of profiles it is necessary to improve the method by adding smoothing procedures. The results obtained with IPMM must be compared carefully to the results of the Integral Method with Fourier Transforms, which is preferred in the case of the triangular grating.

Taking in account these theoretical results, the practical manufacture of the metal grating seems to be a very important procedure due to the fact that the grating period and the groove height strongly affect the intensity of the emitted SP radiation. Using shallow gratings and electron beams with energies up to 10 MeV the theory shows that the intensity of SP radiation will be higher than in the case of deeper gratings and larger electron energies.
The calculated results will offer the possibility to describe the experimental setup in order to investigate the FIR and THz region based on a SP mechanism. Shortening the grating ratio a/D we obtain results with more narrow peaks. It also increases the angle η where the large peak appears.

References

[1] S.J. Smith & E.M. Purcell, Visible light from localized surface charges moving across a grating, Phys.Rev 92, p.1069 (1953)

[2] Douglas J. Paul, Picturing people: non-intrusive imaging, Cavendish Laboratory, University of Cambridge (State of the Science Review), (2003)

[3] P. Rullhusen, X. Artru, P. Dhez, Novel radiation sources using relativistic electrons, Series on S.R. Techniques and Applications, Vol. 4, World Scientific (1998)

[4] J.H. Brownell et al. Improved μFEL performance with novel resonator, Dept. of Physics and Astronomy, Dartmouth College, Hanover, NH USA

[5] Electromagnetic Theory of Gratings, edited by R. Petit, Springer-Verlag, Berlin (1980).

[6] H. Ikuno & K. Yasuura, IEEE Trans. Antennas Propag, Vol. AP-21, No. 5, p.657 (1973)

[7] O. Haeberle et al., Phys. Rev., Vol. 49, No. 4, pp. 3340-3352 (1994).

[8] P. M. Van den Berg, Appl. Sci. Res., Vol. 24, pp. 261-293 (1971).

[9] F. Scarlat et al, NIMB 173 (1-2) 93 (2001) and A. Karabarbounis et al NIMB 173 (1-2) 99 (2001)

[10] "New focus" in Science 8 Feb. 202